Modeling the Thermal Performance of Ballasted Roof Systems

André O. Desjarlais **Thomas W. Petrie** **Jerald A. Atchley**

ABSTRACT

Continuous monitoring for three years documented membrane temperatures and insulation heat fluxes under ballasted roofs and for roofs with exposed white and black membranes. The overall goal of the project was to evaluate how the thermal mass of three different loadings of stone ballast and a heavy paver, all with relatively low solar reflectance, affects energy performance, especially compared to the highly reflective white roof. This paper summarizes the results of the measurements for all three years. They indicate that thermal mass effects are significant for the low R-value roofs in the climate of East Tennessee. Cooling loads for the heavily ballasted systems and the weathered white roof are nearly the same. The lighter ballasts had cooling loads more than the white roof but less than the black roof. The heating loads for the heaviest stone-ballasted system are slightly less than for the black roof. For the paver and the other stone-ballasted systems, heating loads are nearly the same as for the white roof.

An important goal was to predict energy performance with more typical roof insulation levels and in climates different from the test climate. An effort was made to model the energy performance of all six systems in the test climate with the Simplified Transient Analysis of Roofs (STAR) program. For the black roof relative to the white roof, predicted differences in cooling and heating loads were both slightly higher than measured differences. This is consistent with anomalies in the measurements, including the effect of moisture, which STAR did not model.

For the ballasted systems, effective thermal conductivity and specific heat for use in STAR were estimated by trial-and-error, guided by diurnal behavior of the test roofs. For the ballasted roofs relative to the white roof, differences in cooling loads were very similar to those from the measurements as ballast loading and type were varied. The trends continued with higher roof insulation levels and more severe cooling climates than for the measurements. Using these same properties, differences in heating loads were significantly larger than measurements. STAR is too simple a model to predict heating loads for ballasted roofs.

INTRODUCTION

A three-year experimental and analytical study was initiated in March 2004 to quantify the energy performance of ballasted roof systems relative to systems with cool roof membranes. Modeling the energy performance of the ballasted systems was an important goal of the project. The hope was that success could eventually allow ballast to be entered as a roof component in an extension of the DOE Cool Roof Calculator (Petrie *et al.* 2001, Petrie *et al.* 2004). In this calculator, annual heating and cooling loads are estimated for proposed and white roofs in the desired climate. Cooling benefits and heating penalties are then calculated, which allow estimation of operating cost savings.

The study continues and builds upon work performed with the Single Ply Roofing Institute under terms of user agreements for cooperative research (Miller *et al.* 2002, Miller *et al.* 2004, Miller and Roodvoets 2004). Low-slope roof systems were constructed and instrumented for continuous monitoring in the climate of East Tennessee at a U.S. national laboratory. For the heaviest stone loading, the weight per unit area was set equal to that of a heavyweight concrete paver deployed with the stone ballasts. The lightest stone loading

A.O. Desjarlais *is a group leader,* ***T.W. Petrie*** *is a research engineer, and* ***J.A. Atchley*** *is an engineering technologist in the Building Envelopes Group, Engineering Science and Technology Division, Oak Ridge National Laboratory, Oak Ridge, TN.*

was the minimum applied in practice. A third stone ballast weight was half way between the heaviest and lightest. The ballasted systems were installed on the same test building as two systems that acted as controls for the experiment. The unballasted controls exposed a black EPDM membrane and a white TPO membrane. The same black membrane was used under the ballasts.

To monitor energy performance, surface temperature was measured for the exposed membranes and for the membranes under the ballasts. Independently, heat flux was measured through the insulation in all systems. Gillenwater *et al.* (2005) give details on the construction of the test sections and other instrumentation. They present and discuss the measured membrane temperatures and insulation heat fluxes during the first year of monitoring. Desjarlais *et al.* (2006) review the behavior of the membrane temperatures and insulation heat fluxes through two years of monitoring. They conclude that the ballasted systems should be considered for ENERGY STAR® status since their energy performance meets or exceeds that for products that have this status.

This paper summarizes the results of the measurements for all three years in East Tennessee. In anticipation of the modeling effort, the heat fluxes through the insulation are summed with the same constraints as used for summing heat fluxes at the inside surface of the roof for the DOE Cool Roof Calculator. These sums are defined as the measured cooling and heating loads per unit area and are compared for the various roofs.

The modeling effort and results from it are also described, using climatic data obtained along with the energy performance of the various roofs. The effort sought to use the one-dimensional transient heat conduction equation that is programmed in finite difference form in Simplified Transient Analysis of Roofs (STAR) (Wilkes 1989). STAR is the modeling tool used to develop the DOE Cool Roof Calculator. Emphasis is on the effect that different values for the effective thermal conductivity and specific heat of the ballasts have on the diurnal behavior of the predictions. For direct comparison to measured cooling and heating loads, cooling and heating loads of the various roofs are then predicted with properties that duplicate the measured diurnal behavior.

MEASURED HEAT FLUXES, COOLING LOADS AND HEATING LOADS

Figure 1 is a sketch of the stone-ballasted systems constructed for this project. With pavers instead of stone, it shows the layout of the paver-ballasted system. With no ballast and an exposed white or black membrane, it applies to the control systems. Each system occupied half of a 4 ft x 8 ft (1.2 m x 2.4 m) area on the roof of an outdoor test building in East Tennessee. The light loading and medium loading of stone shared one test section, the heavy loading of stone and the paver shared another, and the exposed white and black membrane systems shared a third.

All test sections were insulated and instrumented identically. Pairs of thermocouples were located under all membranes, between the pieces of wood fiberboard insulation and on top of the deck. The fiberboard provided thermal resistance of R-3.8 (RSI-0.67). For each ballasted system, two thermocouples were also located near the outside surface of the ballast. A heat flux transducer was put between the pieces of wood fiberboard in the center of each test section.

A data acquisition system did continuous monitoring of the output from the thermocouples, heat flux transducers and instrumentation in a weather station above the roof of the test building. The experimental work included the initial and subsequent occasional measure of the solar reflectance of all exposed surfaces, an estimate of their infrared emittance, weekly analysis of temperature and heat flux data, and weekly comparison of the temperatures and heat fluxes for the ballasted and control systems.

Figure 2 presents the average weekly heat fluxes through the insulation in each system over the course of the project. The light, medium and heavy loadings of stone ballast are identified by 10#, 17# and 24#, respectively. The three cooling seasons in the project are shown as the intervals from 4/20/2004 through 10/19/2004 (summer 2004), 4/21/2005 through 10/20/2005 (summer 2005), and 4/22/2006 through 10/21/2006 (summer 2006). The three heating seasons are 10/20/

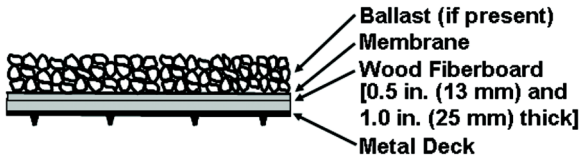

Figure 1 *Layers in a typical ballasted system.*

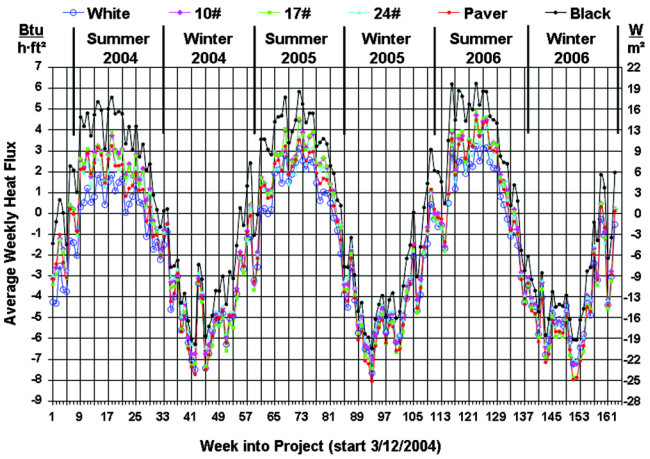

Figure 2 *Average weekly heat fluxes for the ballasted and control systems over the three year duration of the project.*

2004 through 4/20/2005 (winter 2004), 10/21/2005 through 4/21/2006 (winter 2005) and 10/22/2006 through 4/22/2007 (winter 2006).

The average weekly heat flux for the black system is generally the highest (largest positive number) for all systems each week during the summers. It is generally the smallest (smallest negative number) during the winters. The average weekly heat flux for the white system is generally the lowest during the summers, especially the first summer. Complete weathering of the TPO membrane for the white system is achieved by the start of the second summer. It is difficult to distinguish any difference among the average weekly heat fluxes for the ballasted systems during the summers. There is little difference among the average weekly heat fluxes for the ballasted systems and the white system during the winters.

Not shown in Figure 2 are data for two paver systems with heavy and medium loading that occupied a fourth area on the test facility beginning in Summer 2005. These pavers were painted with a white coating that yielded solar reflectance slightly greater than that of the white membrane before weathering. They had average weekly heat fluxes lower than the white control during the cooling seasons. They behaved the same as the other ballasted systems during the heating seasons. This is expected behavior for systems that combine the effects of high solar reflectance and high thermal mass. They are not discussed further in this paper because neither was the usually installed paver system.

The data from which Figure 2 was prepared were further analyzed in anticipation of the effort to model the energy performance of the ballasted systems. The usefulness of this modeling is to compare proposed systems to a white system for roof insulation levels and climates different from those for the side-by-side tests. In comparisons that are done in the DOE Cool Roof Calculator (Petrie *et al.* 2001, Petrie *et al.* 2004), cooling loads are defined as the annual sum of the positive heat fluxes through the roof deck when outside air temperature is greater than 75°F (23.9°C). Heating loads are defined as the sum of the negative heat fluxes through the roof deck when outside air temperature is less than 60°F (15.6°C). Not including the small heat fluxes between 75°F (23.9°C) and 60°F (15.6°C) is meant to approximate the dead band, at least that due to the roof, when the building under the roof needs neither heating nor cooling.

These definitions were applied to the heat fluxes through the insulation for the three years. Using the insulation heat fluxes instead of deck heat fluxes was necessary because deck heat fluxes were not measured. Most of the annual cooling loads occurred during the summers defined in Figure 2 and most of the annual heating loads during the winters. This arbitrary division of each year into two seasons was to generate smaller worksheets for organization and manipulation of the data. A summary worksheet combined the summer and winter results for each year.

Cooling and heating loads for the white system are shown in Table 1. Even for this relatively simple system, changes in climatic conditions from year to year and changes in the system itself make for complicated behavior. Loads for white systems are affected by the change in solar reflectance of the surface. For this TPO membrane, the decrease in its solar reflectance due to weathering was complete by the start of the second year. This may explain part of the increase in cooling load from the first year to the second. The increase in heating load must be weather-related. Moreover, the loads for the second and third year would have been the same had climatic conditions not changed.

Figures 3 and 4 give more detail than Figure 2 about the energy performance of the black and ballasted systems relative to the white system. For Figure 3, the cooling load for the white system was subtracted from the corresponding cooling load for each proposed system in each year. Positive numbers mean more cooling load than the white system. The black system behaves as expected. It has the largest cooling load relative to the white system. The difference decreases as the white membrane weathers. The thermal mass associated with the heavy loadings makes them perform as well for cooling as the white system in the mixed climate of East Tennessee. The light and medium loadings are both better than the black system but do not have as much cooling benefit as the white system.

For Figure 4, the heating load for each proposed system was subtracted from the corresponding heating load for the white system in each year. Positive numbers mean the proposed system has more heating load than the white system. The results for the black system are as expected. Its energy advantage over a white system is less heating load, which decreases as the white membrane weathers. The ballasted systems show no clear trends. As Figure 2 showed, there is little difference among the ballasted and white systems during the winters. Figure 4 shows that, when only the negative heat

Table 1. Measured Cooling and Heating Loads for the White Roof Compared to Heating and Cooling Degree-Days over the Three Years of the Project

Year of Project	Cooling Load Btu/·ft² (kJ/m²)	Cooling Degree-Days [°F(°C)-day]	Heating Load Btu/ft (kJ/m²)	Heating Degree-Days [°F(°C)-day]
2004	6960 (79020)	1502 (834)	-22220 (-252290)	3614 (2008)
2005	9340 (106020)	1672 (929)	-23740 (-269620)	3947 (2193)
2006	8790 (99800)	1560 (867)	-24740 (-280990)	4187 (2326)

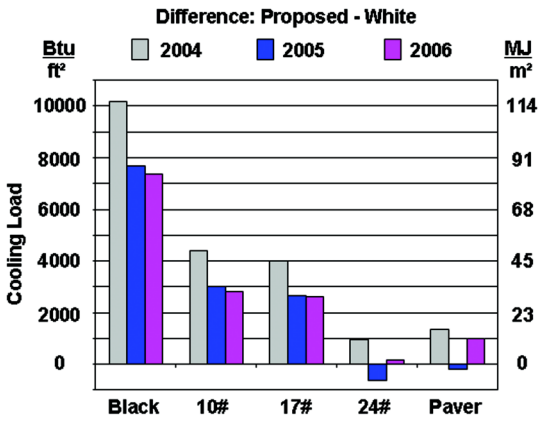

Figure 3 *Differences in cooling loads between the proposed and white systems during the years of the project.*

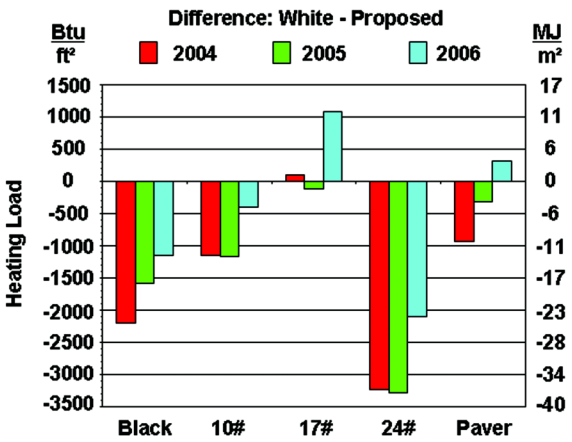

Figure 4 *Differences in heating loads between the white and proposed systems during the years of the project.*

fluxes are used for the heating load, unlike both positive and negative heat fluxes to get the average for each week in Figure 2, there is little difference among heating loads for all these systems, including the black system. Only the 24# system shows less heating load than the black system due to the effect of thermal mass.

Figures 3 and 4 apply only to the low R-value roofs for the changing climatic conditions in East Tennessee during the three years of the project. They provide experimental evidence that neither the cooling loads nor the heating loads are much different for the four ballasted systems and the white system. This supports the conclusion of Desjarlais, *et al.* (2006) after two years. Possible operating cost savings with ballasted systems compared to white systems depend not only on the heating and cooling loads, but also on the efficiency of the heating, ventilating and cooling equipment and the price of energy to run it.

PROPERTIES NEEDED TO PREDICT ENERGY PERFORMANCE WITH STAR

To fulfill the goals of the project, an effort was made to model the behavior of the ballasted and control systems shown in Figures 2, 3 and 4. Because of its use for the DOE Cool Roof Calculator and our extensive experience with it, the program STAR was chosen. It is a finite-difference form of the transient heat conduction equation in one dimension and allows all three types of boundary conditions at the inside and outside surfaces of a low-slope roof system. The temperature measured at the top of the deck was used as the inside boundary condition. Data from the weather station on the test facility were used to impose convection and thermal radiation as the boundary condition at the outside of each system.

STAR also requires a layer by layer description of the physical and thermal properties of roof systems. The physical layout of the systems was shown in Figure 1. Table 2a lists the properties for initial runs of STAR. Data are listed for the three loadings of stone (10#, 17# and 24#), the paver, the exposed white and black membranes, and the two layers of wood fiberboard insulation that are used in each system.

Direct measurements were made of the thickness and density of the various components of the systems. The weight of several pavers was measured by a scale and divided by the measured volume to yield density. A nominal 5-gallon (18.9 L) bucket was weighed, filled with stone and weighed again. The actual volume of the bucket was determined by measuring the weight of water to fill it. Weight of stone divided by its volume yielded the average density of the stone including air spaces. The weight of water to fill the spaces around the stones yielded a porosity of 40%.

Table 2a includes the ranges of solar reflectance for all surfaces. Table 2b gives seasonal variation for the exposed smooth surfaces (white and black membranes and paver). Averages are presented for summer 2004 through winter 2006 and prove that changes due to weathering are essentially complete by the beginning of summer 2005. Solar reflectance was measured at about six month intervals during the project according to ASTM C 1549-02: Standard Test Method for Determination of Solar Reflectance Near Ambient Temperature Using a Portable Solar Reflectometer. The solar reflectance of the stone was measured at the beginning of each year of the project according to ASTM E 1918-97: Standard Test Method for Measuring Solar Reflectance of Horizontal and Low-Sloped Surfaces in the Field. (See the Acknowledgement.) All the exposed surfaces are non-metallic solids for which the infrared emittance is taken to be 0.9 from previous measurements and experience (Petrie et al. 2001).

The thermal conductivity and specific heat of the white and black membranes and the fiberboard were obtained from the literature and our own measurements. For the stone and pavers, the program Properties Oak Ridge (PROPOR) was used as part of the ongoing analysis of the evolving data to estimate effective thermal conductivity and volumetric heat

Table 2a. Properties Input to STAR for Initial Modeling of the Ballasted and Control Systems

	10#	17#	24#	Paver	White	Black	Fiberboard
Loading, lb/ft (kg/m²)	10.0 (49)	16.9 (82)	23.9 (117)	23.5 (115)	negl.	negl.	n.a.
Thickness, in. (mm)	1.3 (33)	2.2 (56)	3.1 (79)	2.0 (51)	0.050 (1.3)	0.045 (1.1)	0.5, 1.0 (13, 25)
Thermal conductivity, Btu·in./(h·ft²·°F) [W/(m·K)]	6.21 ±6 (0.90±0.9)	5.94 ±7 (0.86±1)	4.65 ±2 (0.67±0.3)	17.6 ±4 (2.5±0.6)	1.2 (0.17)	1.2 (0.17)	*a+b·T
Density, lb/ft³ (kg/m³)	92.4 (1480)	92.4 (1480)	92.4 (1480)	141 (2260)	58 (930)	58 (930)	17.5 (280)
Specific heat, Btu/(lb·°F) [kJ/(m·K)]	0.17 ±0.2 (0.71±0.8)	0.21 ±0.3 (0.88±1.3)	0.20 ±0.1 (0.84±0.4)	0.15 ±0.04 (0.63±0.17)	0.4 (1.7)	0.4 (1.7)	0.19 (0.80)
Infrared emittance, %	90	90	90	90	90	90	not needed
†Solar reflectance, %	20	20	20	54 to 47	71 to 60	8 to 9	not needed

* From guarded hot plate measurements: kfiberboard [Btu·in./(h·ft²·°F)] = 0.3376 + 0.000746·T(°F); kfiberboard [W/(m·K)] = 0.05213 + 0.0001936·T(°C)
† Ranges, if given, span observed variation over the three years of the project

Table 2b. Variation of Solar Reflectance for the Smooth Surfaces in the Project

Solar Reflectance, %	Summer 2004	Winter 2004	Summer 2005	Winter 2005	Summer 2006	Winter 2006
White TPO	70.5	63.7	61.8	60.4	60.7	60.5
Black EPDM	8.0	8.9	9.4	9.1	9.0	8.8
Paver	54.0	52.0	49.4	49.3	48.9	47.2

capacity (the product of density and specific heat). PROPOR compares the temperatures and heat fluxes that are measured inside a system to those predicted by the transient heat conduction equation. Temperatures measured at the outside and inside surfaces are boundary conditions. Thermal conductivity and volumetric heat capacity are considered parameters. Values of the parameters are adjusted by an automated iteration procedure until best agreement is obtained. Best agreement is defined as the minimum of the squares of the differences between measured and predicted temperatures and heat fluxes inside the systems. An estimate of the confidence in the final parameter values is included as part of the output from the program (Beck *et al.* 1991).

Use of PROPOR, which like STAR is based on a finite-difference form of the transient heat conduction equation, indicated that modeling the energy performance for the ballasted systems is more difficult than for the black and white systems. PROPOR had difficulty converging to estimates of the thermal conductivity and volumetric heat capacity for the 10# and 17# loadings of stone except for several weeks during each winter in East Tennessee. Even then the estimates were not acceptably precise. Convergence for the 24# loading was less difficult. Convergence was obtained for the paver no matter what the weather conditions.

One reason for the problems with convergence and lack of confidence is convection effects in the lighter weights of stone during high solar loading. Another reason is inaccurate measurement of outside surface temperatures for all the ballasts. Unlike STAR, PROPOR requires temperatures at the surface as the only allowed type of boundary condition. For the ballasts, thermocouple measuring junctions were placed against two stones at the top of each stone loading and slightly below the outside surface of the central paver (Gillenwater *et al.* 2005). Unreliable surface temperatures are more likely for the light loadings of stone when the sun is high in the sky. Sunlight can penetrate to the black membrane and cause it to heat the stones from below.

The thermal conductivity and specific heat for the stone and paver in Table 2a are the averages of estimates from PROPOR for weeks when it converged. The uncertainty reported by PROPOR is appended to these estimates. Specific heat is obtained by dividing the estimated volumetric heat capacity by the measured density. Only the volumetric heat capacity is used by PROPOR and by STAR. The uncertainties in the estimates for both properties of the stone are of the order of 50% to 150% of the estimates themselves. Furthermore, the effective thermal conductivity and, to a lesser extent, the specific heat vary with the stone loading. This would not be true if heat transfer through the stone were strictly a heat conduction phenomenon, or at least apparent thermal conduction, like conduction and radiation in mass insulation. The

three loadings were obtained with the same stone; only thickness of application was changed.

The 0.19 to 0.24 Btu/(lb·°F) [0.80 to 1.00 kJ/(kg·K)] range for specific heat of heavyweight concrete (ASHRAE 2005) and the specific heat of 0.24 Btu/(lb·°F) [1.00 kJ/(kg·K)] for air compare well to values for the ballast in Table 2a. ASHRAE handbook values of the thermal conductivity of heavyweight concrete are given as the range from 9.0 to 18.0 Btu·in./(h·ft²·°F) [1.3 to 2.6 W/(m·K)], which includes the value for the paver in Table 1. Possible values for the thermal conductivity of the stone are given by Côté and Konrad (2005). The porosity of the stone was measured as 40%. Côté and Konrad's data for granite and limestone show a thermal conductivity of 1.80 Btu·in./(h·ft²·°F) [0.26 W/(m·K)] at this porosity, 29 to 39% of the values for the stone ballasts in Table 2a.

An attempt was made to measure the thermal conductivity at 75°F (24°C) of the stone and paver by ASTM C518-98: Standard Test Method for Steady-State Heat Flux Measurements and Thermal Transmission Properties by Means of the Heat Flow Meter Apparatus. Samples of the stone and paver were sandwiched between pieces of foam to protect the apparatus and provide the required level of thermal resistance. The foam used was characterized separately. Differences between R-values and thicknesses with and without the stone yielded stone sample thermal conductivity of 1.86 Btu·in./(h·ft²·°F) [0.27 W/(m·K)] for heat flow up and 1.76 Btu·in./(h·ft²·°F) [0.25 W/(m·K)] for heat flow down. The average agrees exactly with the data from Côté and Konrad. Slightly higher thermal conductivity for heat flow up is consistent with the effect of air between the individual stones. By the same technique, the solid paver had thermal conductivity of 6.58 Btu·in./(h·ft²·°F) [0.95 W/(m·K)], 27% of the value in Table 2a.

DIURNAL BEHAVIOR OF MEASUREMENTS AND OF PREDICTIONS USING INITIAL ESTIMATES OF PROPERTIES

STAR was executed with the properties in Table 2a and Table 2b, yielding predictions of membrane temperatures and insulation heat fluxes for all three years of the project. The thermal conductivity and specific heat in Table 2a for the ballasts were considered initial values. Because of the large uncertainty of their estimation by PROPOR and the low values of thermal conductivity indicated by the literature and the C518 measurements, it was unlikely that they would yield acceptable agreement with measurements. A trial-and-error process was anticipated to select final values. Modeling the behavior of the exposed white and black membrane systems was straightforward.

Hourly predicted membrane temperatures and insulation heat fluxes were entered in a spreadsheet that contained the hourly averages of the measurements. Graphs could then be generated for selected days to show diurnal behavior and indicate agreement between measurements and predictions. Clear days show maximum solar effect and have smooth curves through the hourly temperatures and heat fluxes. There are few deviations caused by cloudiness and inclement weather that make it difficult to visually compare the data. Figure 5 shows a typical clear day during the first summer of the project when the solar reflectance of the white surface was highest.

The black and white systems are lightweight systems with R-3.8 (RSI-0.67) fiberboard insulation. The ballasted systems are thermally massive with the same insulation. Table 2a and our measurements of apparent thermal conductivity with ASTM C 518 yield additional R-value of R-0.7 (RSI-0.13), R-1.2 (RSI-0.21), R-1.7 (RSI-0.3) and R-0.3 (RSI-0.05) for the 10#, 17#, 24# and paver ballasts, respectively. Figure 5 shows that peak values of the measured membrane temperature and

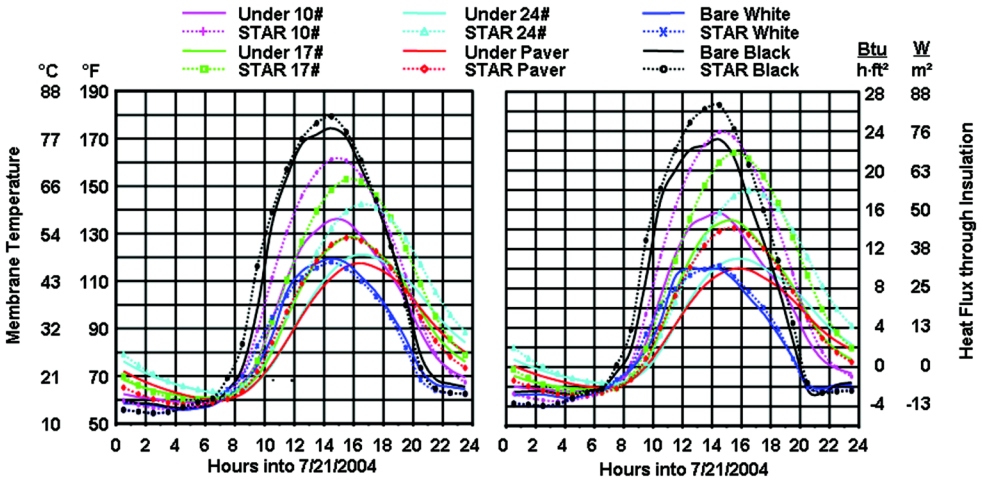

Figure 5 *Diurnal behavior of measurements and predictions using properties in Tables 2a and 2b for a typical clear day during the project.*

insulation heat flux and the time when peaks occur are affected by the thermal mass and extra R-value of the ballasts. The 24# system with 20% solar reflectance has the same peak values as the 70% reflective white system. The 54% reflective paver has smaller peak values.

The time at which peak heat flux occurs is important to operation of the building under a low-slope roof system. The ballasted systems show consistent delays relative to the black and white systems. For ten clear days over the course of the project, including the example day for Figure 5, the average times of peak heat flux for the white and black systems coincide within 0.4 h. Relative to the black system, the 10#, 17#, 24# and paver systems show peak heat fluxes delayed by 0.9 h, 1.8 h, 2.7 h and 2.4 h, respectively. This variation agrees with the variation of the loading of the respective systems in Table 2a. This proves that the ballasted systems show significant and consistent effect of their thermal mass. The delays are not consistent with added R-value.

The relatively simple behavior of exposed white and black membranes over a low-slope roof with low thermal mass is well understood from previous experience with test sections used to validate STAR for the DOE Cool Roof Calculator (Petrie 2001). On the several clear days the hourly predictions for the exposed white membrane were in good agreement with the measurements and consistent with our understanding. The hourly behavior of the exposed black membrane, when compared to that from previous experience, indicates that the measured temperatures are accurate but the measured heat fluxes are low. Temperatures and heat fluxes were measured independently with thermocouples and small heat flux transducers, respectively. More uncertainty in measured heat fluxes is consistent with our experience. It occurs despite calibration of the heat flux transducers in the wood fiberboard insulation according to ASTM C 518.

The shape of the predicted curves on the clear days was correct for the control systems, with low thermal mass and either an exposed white or black membrane. Predicted peak times coincided with the measured peak times. The nighttime predictions were generally low for both these controls. This is likely due to the effects of condensation and no attempt was made to model its effect.

Regarding the diurnal behavior of the predictions of membrane temperature and insulation heat flux for the ballasted systems with properties in Table 2a, peak times generally coincided with the measured peak times. Agreement in early morning between predictions and measurements was acceptable for the stone ballasts but not for the paver. However, predicted peak values for all ballasted systems were higher than the corresponding peak measurements. This is the dominant feature of Figure 5 and precludes having any confidence in the accuracy of the predictions, night or day, using the set of properties in Table 2a.

DIURNAL BEHAVIOR USING FINAL ESTIMATES OF PROPERTIES

Trials, in which density was held at the measured values, indicated that peak times are most sensitive to specific heat. If specific heat is increased, peak time is delayed. Peak values are most sensitive to thermal conductivity. If thermal conductivity is decreased, the peak membrane temperature and insulation heat flux also decrease. However, changes in specific heat affect peak values and changes in thermal conductivity affect peak times to some extent. STAR was executed with thermal conductivity values for the stone and paver that were varied as a percentage of the values in Table 2a. Specific heat was varied less, seeking a common value for the stone.

The best overall agreement between predictions and measurements was judged to occur for thermal conductivity corresponding to 10%, 15%, 20% and 20% of Table 2a values for the 10#, 17#, 24# and paver systems, respectively. These values are 34% to 53% of the values measured by ASTM C518. The specific heat for the stone was chosen to be 0.10 Btu/(lb_m·°F) [0.42 kJ/(kg·K)]. For the paver 0.21 Btu/(lb_m·°F) [0.88 kJ/(kg·K)] was chosen. The ASHRAE Handbook of Fundamentals (ASHRAE 2005) lists 0.19 to 0.24 Btu/(lb_m·°F) [0.80 to 1.00 kJ/(kg·K)] as the range for heavyweight concretes, yielding a geometric mean of 0.21 Btu/(lb_m·°F) [0.88 kJ/(kg·K)]. Table 3 lists the complete set of property values. Table 2b was again used for the seasonal variation of solar reflectance of the smooth surfaces.

Figure 6, for the same typical day chosen for Figure 5, shows the much improved agreement between predictions and measurements for the ballasted systems when the properties in Table 3 are used. Predictions for the controls are unchanged. Predicted peak temperatures and heat fluxes for all ballasts agree very well with measurements. Predicted peak times for the stone ballasts do not coincide exactly with the observed peak times, because the same specific heat was imposed for all three stone ballasts.

Generally, for all days and all ballasts, there are anomalies in the measurements that a model like STAR, with relatively few parameters, cannot duplicate. Many of them are associated with moisture effects that STAR did not model. Dew or frost persisted on the exposed membranes well into mid-morning of many days. It was noticed that the test sections on the lower end of the low-slope roof of the test building, namely, the black control, the 10# system and, to a lesser extent, the paver, retained water for a day or more after rain events. Rain drained quickly from the other test sections on the higher end of the roof.

COMPARISON OF COOLING AND HEATING LOADS FROM PREDICTIONS AND MEASUREMENTS

As explained above, final estimates were made by trial-and-error of the effective thermal conductivity and specific heat needed to model the diurnal behavior of the ballasted systems with the transient heat conduction equation. To test their usefulness, cooling and heating loads were generated

Table 3. Properties Input to STAR for Final Modeling of the Ballasted and Control Systems

	10#	17#	24#	Paver	White	Black	Fiberboard
Loading, lb/ft² (kg/m²)	10.0 (49)	16.9 (82)	23.9 (117)	23.5 (115)	negl.	negl.	n.a.
Thickness, in. (mm)	1.3 (33)	2.2 (56)	3.1 (79)	2.0 (51)	0.050 (1.3)	0.045 (1.1)	0.5, 1.0 (13, 25)
Thermal conductivity, Btu·in./(h·ft²·°F) [W/(m·K)]	0.621 (0.090)	0.891 (0.129)	0.930 (0.134)	3.52 (0.508)	1.2 (0.17)	1.2 (0.17)	*a+b·T
Density, lb/ft³ (kg/m³)	92.4 (1480)	92.4 (1480)	92.4 (1480)	141 (2260)	58 (930)	58 (930)	17.5 (280)
Specific heat, Btu/(lb·°F) [kJ/(m·K)]	0.10 (0.42)	0.10 (0.42)	0.10 (0.42)	0.21 (0.88)	0.4 (1.7)	0.4 (1.7)	0.19 (0.80)
Infrared emittance, %	90	90	90	90	90	90	not needed
†Solar reflectance, %	20	20	20	54 to 47	71 to 60	8 to 9	not needed

* From guarded hot plate measurements: kfiberboard [Btu·in./(h·ft²·°F)] = 0.3376 + 0.000746·T(°F); kfiberboard [W/(m·K)] = 0.05213 + 0.0001936·T(°C)
† Ranges, if given, span observed variation over the three years of the project

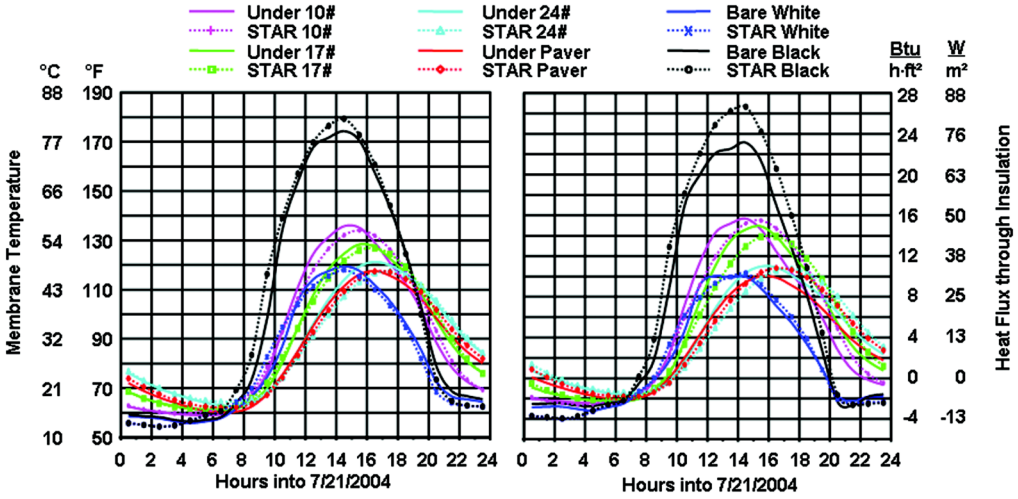

Figure 6 *Diurnal behavior of measurements and predictions using properties in Tables 3 and 2b for a typical clear day during the project.*

using the values in Tables 3 and 2b. The resulting differences for cooling loads are added to Figure 3 to produce Figure 7. The resulting differences for heating loads are added to Figure 4 to produce Figure 8.

The predicted differences in Figure 7 for the ballasted systems are closer to the corresponding measured differences than are predicted and measured differences for the black system. As mentioned in the discussion of Figure 5, the measured heat flux for the black system is lower than previously measured with black systems. The predictions for the black system are considered accurate. Note how well the variation in the measured differences is predicted for all systems from year to year. For the stone ballasts, the use of an effective thermal conductivity that decreases with increased loading, as shown in Table 3, accounts for the solar effects during cooling seasons. The differences between cooling loads for the ballasted systems and the white system are small, but appear to be predicted accurately as a function of ballast loading and ballast type.

As Figure 8 shows, the predicted differences in heating loads for the ballasted systems using properties in Table 3 are significantly larger than the measured differences. A 92% reduction on average would yield exact agreement with the measured differences. A reduction of only 58% on average results if the thermal conductivities in Table 2a are used along with a specific heat of 0.10 Btu/(lb_m·°F) [0.42 kJ/(kg·K)] for all ballasts. Reduction of the specific heat to 0.01 Btu/(lb_m·°F) [0.042 kJ/(kg·K)] decreases the differences another 11%, but

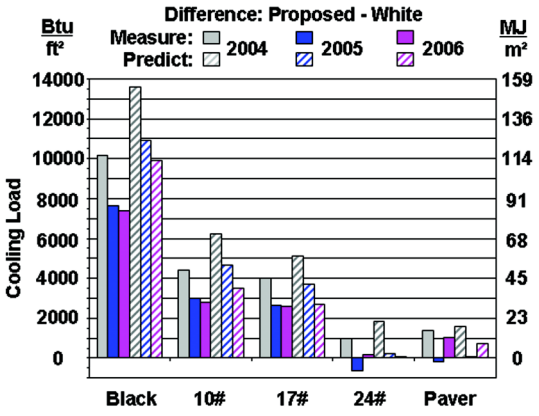

Figure 7 *Differences in cooling loads between the proposed and white systems during the years of the project. Predictions use properties in Tables 3 and 2b.*

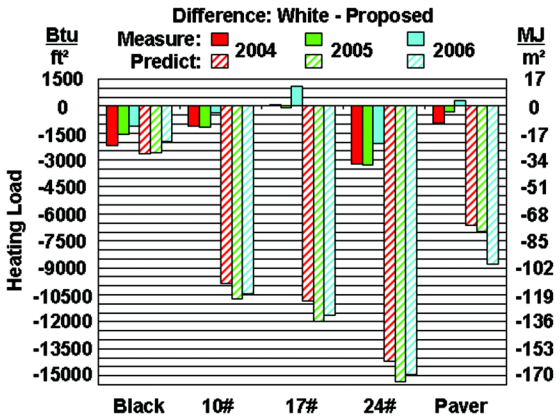

Figure 8 *Differences in heating loads between the white and proposed systems during the years of the project. Predictions use properties in Tables 3 and 2b.*

is physically impossible. Thermal conduction alone is too simple a mechanism to use to predict the heating load of the ballasted systems.

The saving fact remains that the measured differences in heating load between the white system and the ballasted systems are small and random. Predicted heating loads for the white system can serve for the heating loads of ballasted systems, except the 24# system, with uncertainty given by the variation of the measured differences about zero. Predicted heating loads for the black system can substitute for those of the 24# system, duplicating the measured heating loads with no more uncertainty than using the white system for the other ballasts.

COOLING LOADS FOR VARYING INSULATION AND LOCATION

The procedures used to develop the DOE Cool Roof Calculator (Petrie, *et al.* 2001) were applied to the ballasted systems in this project. STAR was run for climates from Anchorage to Phoenix. Ballast properties in Table 3 were used and roof insulation level was varied from R-5 (RSI-0.88) to R-32 (RSI-5.6). Cooling loads were generated from the hourly output and were then fit as a function of location-dependent cooling index and R-value for each system. Fits from the calculator were used for two white systems. The best white system has a solar reflectance of 70%. The worst white system has a solar reflectance of 48%, observed for weathered coatings (Petrie, *et al*. 2001).

Figure 9 compares annual cooling loads for three different locations and three different levels of insulation in the roofs. The test situation is R-5 (RSI-0.88) roof insulation in Oak Ridge Year 1. R-11 (RSI-1.9) and R-19 (RSI-3.3) are required by California Title 24 for nonresidential buildings. As expected the cooling loads decrease almost linearly with increasing insulation R-value at each location. The California climate zone 12 (CZ12) weather file has 12% fewer cooling degree-days and 36% more average solar insolation than Oak Ridge. This results in slightly larger cooling loads than in Oak Ridge. The California climate zone 15 (CZ15) weather file has 194% more cooling degree-days than Oak Ridge and 46% more average solar insolation. This desert climate causes very much larger cooling loads than in Oak Ridge. For any R-value and location, the cooling loads for the ballasted systems, except the 10# system, are between those for the best and worst white systems. In year 1 the white control system in this project had the solar reflectance of the best white system. For the last half of the project its weathered reflectance was half-way between that of the best and worst white systems. The ballasted systems, except the 10# system, have about the same cooling load as such a system regardless of location or level of roof insulation.

CONCLUSIONS

Three full years of continuous monitoring in the mixed climate of East Tennessee yielded data to compare the energy performance of four ballasted systems and a system with an exposed black membrane to that of a system with an exposed white membrane. Heat fluxes through the insulation in each test section were used to obtain the annual cooling and heating loads due to unit area of each system. The cooling loads for the heavy weight stone and paver ballast were approximately the same as for the white system. Cooling loads for the light and medium weight stone systems were slightly larger than for the white system but significantly less than for the black system. Only the cooling load of the white system showed the effects of weathering, which was complete by the start of the second year of the project. Heating loads for the ballasted systems showed random variation as loading increased and type changed. Except for the heavy weight stone system, they were about the same as for the

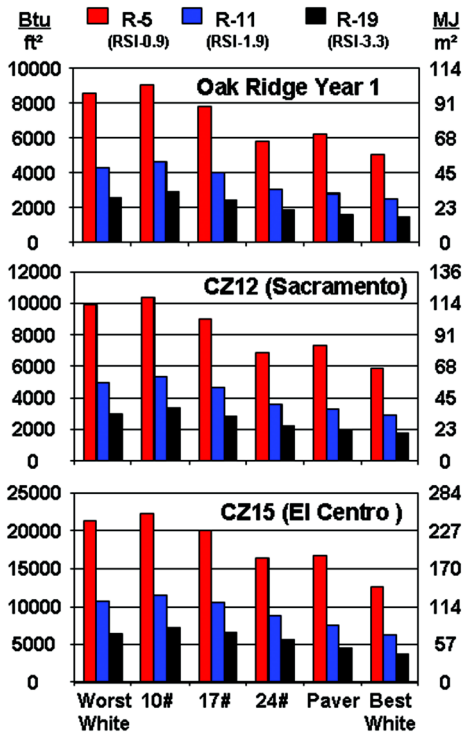

Figure 9 *Cooling loads as a function of roof insulation level in Oak Ridge year 1, California climate zone 12 (Sacramento) and climate zone 15 (El Centro).*

white system. The heavy weight stone system had slightly less heating load than the black system.

An effort was made to model internal heat flow for the ballasted systems with transient heat conduction alone, using the program STAR. STAR has successfully modeled non-ballasted systems in past projects and did so again in this project. Trial-and-error was required to duplicate diurnal variation of measured membrane temperatures and insulation heat fluxes on clear days for the ballasts. Effective thermal conductivities about 30% to 50% of measured values resulted for the stone and paver, along with specific heats close to literature values. With these properties, the predicted cooling loads showed the same variation with ballast loading and type as the measurements. Predictions of cooling loads were made using the procedures of the DOE Cool Roof Calculator for higher levels of roof insulation and more severe cooling climates than for the measurements. Ballasted systems performed relative to white systems like they did in the measurements.

Contrary to the measurements, these properties predicted heating loads for the ballasts much smaller than heating loads for the white system. High effective thermal conductivities and unrealistically low specific heats still did not yield heating loads like the measurements. It is concluded that transient heat conduction alone is not adequate to predict heating loads for ballasts.

ACKNOWLEDGMENTS

The measurement of the solar reflectance of the stone ballasts was done at the start of each year of the project with an apparatus designed by Ross H. Robertson of the Firestone Building Products Company. Ross brought it to Oak Ridge to assist with the measurements. He also suggested the use of coated pavers to observe the effect of simultaneous use of high solar reflectance and high thermal mass. Ross had the pavers coated and helped to deploy them at the start of the second year of the project when space became available on the test building. His death near the end of the project meant he could not see the results of this project and lend his insights to conclusions from it. He always carried out projects diligently and thoroughly. He will be missed as a colleague and a friend.

REFERENCES

ASHRAE. 2005. "2005 ASHRAE Handbook: Fundamentals," Chapter 25, Table 4; Chapter 39, Table 3. Atlanta: American Society of Heating, Refrigerating and Air Conditioning Engineers, Inc.

Beck, J.V., Petrie, T.W. and Courville, G.E. 1991. "Using Parameter Estimation to Analyze Building Envelope Thermal Performance," pp. 161-191, Special Report 91-3. In-Situ Heat Flux Measurements in Buildings: Applications and Interpretations of Results. S.N. Flanders, Editor. Hanover, NH: U.S. Army Cold Regions Research and Engineering Laboratory.

Côté, J. and Konrad, J-M. 2005. "Thermal Conductivity for Base-Course Materials," pp. 61-78, *Canadian Geotechnical Journal,* vol. 42, no. 11.

Desjarlais, A., Petrie, T., Miller, W., Gillenwater, R., and Roodvoets, D. 2006. "Evaluating the Energy Performance of Ballasted Roof Systems," for presentation and publication in the proceedings, 3rd International Building Physics Conference, Montreal, August 27-31, 2006.

Gillenwater, Dick, Petrie, Tom, Miller, Bill, and Desjarlais, Andre. 2005. "Are Ballasted Roof Systems Cool?" presented at Roof Consultants Institute May 2005 Conference "Cutting Through the Glare" and published in pp. 32-44, *RCI Interface*, vol. XXIII, no. 9 (September 2005).

Miller, W.A., Cheng, M.D., Pfiffner, S. and Byars, N. 2002. "The Field Performance of High-Reflectance Single-Ply Membranes Exposed to Three Years of Weathering in Various U.S. Climates," August 2002 Final Report to SPRI, Inc.

Miller, W.A. and Roodvoets, D. 2004. "Saving Energy by Cleaning Reflective Thermoplastic Low-Slope Roofs," in proceedings of *Performance of Exterior Envelopes of Whole Buildings IX.* Atlanta: American Society of Heating, Refrigerating and Air Conditioning Engineers, Inc.

Miller, W.A., Roodvoets, D.L. and Desjarlais, A. 2004. "Long Term Reflective Performance of Roof Membranes," in proceedings of the 2004 Roof Consultants Institute Convention.

Petrie, T.W., Atchley, J.A., Childs, P.W. and Desjarlais, A.O. 2001. "Effect of Solar Radiation Control on Energy Costs – A Radiation Control Fact Sheet for Low-Slope Roofs," in proceedings of *Performance of the Exterior Envelopes of Whole Buildings VIII: Integration of Building Envelopes*. Atlanta: American Society of Heating, Refrigerating and Air-Conditioning Engineers, Inc.

Petrie, T.W., Wilkes, K.E. and Desjarlais, A.O. 2004. "Effect of Solar Radiation Control on Electricity Demand Costs–an Addition to the DOE Cool Roof Calculator," in proceedings of *Performance of Exterior Envelopes of Whole Buildings IX*. Atlanta: American Society of Heating, Refrigerating and Air Conditioning Engineers, Inc.

Wilkes, K.E. 1989. "Model for Roof Thermal Performance." Report ORNL/CON-274. Oak Ridge, TN: Oak Ridge National Laboratory.